

OPTICAL EFFECTS OF ENERGY DEGRADERS ON THE PERFORMANCE OF FRAGMENT SEPARATORS

L. Bandura[#], B. Erdelyi, ANL, Argonne, IL 60439, U.S.A. and NIU, DeKalb, IL 60115, U.S.A.
J. Nolen, ANL, Argonne, IL 60439, U.S.A.

Abstract

Next-generation facilities for the production of exotic beams require large acceptance fragment separators to separate and transmit rare isotopes. Fragment separators require energy degraders in order to achieve high purity separation of these rare species. The introduction of the degrader into an aberration-free optical design of a separator induces aberrations at the achromatic image. These may be completely eliminated by shaping the degrader appropriately. We have shown that, in order to eliminate these aberrations, some aberrations must be nonzero at the dispersive image, where the degrader is placed. A second order design with robust optics is presented.

INTRODUCTION

There are many next-generation facilities for the production of exotic beams that are currently under commissioning, construction, or envisioned for the future [1-7]. These facilities will produce rare isotopes in large quantities and fragment separators will be required in order to capture, separate, and transport the beam to experimental stations for study. In order to achieve high separation purity, the fragment separator must consist of several achromatic imaging stages which are free of aberrations.

Since electromagnetic fields alone will not separate isotopes, energy degraders must be used. This method of separation is called the “ $B\rho$ - ΔE - $B\rho$ ” method and takes advantage of the fact that isotopes with different mass and charge lose different amounts of energy in the degrader. To select one isotope from the beam, the degrader is shaped to focus only that isotope at the achromatic image. Here we will show that, if the optics are designed to be aberration-free to second order at the achromatic image without the energy degrader, then the addition of the degrader will not spoil the image if it is shaped appropriately. A future paper, currently in preparation, will give a comprehensive analysis of energy degraders [9]. This paper will highlight many higher order optical effects not presented here.

The fragment separator design presented here is based on several symmetry theories described in [8]. The design specifications require a layout with large acceptance (40 cm in x and 20 cm in y), due to the large emittances that result from the nuclear reactions in the target. Also, the design should have high transmission and resolution. Table 1 shows the parameters of the

focusing elements and drifts in the fragment separator design. The dipoles, required for rigidity selection, have a radius of curvature of 5 m and an angle of 35 degrees. Figure 1 shows the optical layout along with the beam envelope.

Table 1: Parameters of fragment separator optics. These magnet strengths are needed to focus a 370 MeV/u ^{132}Sn beam. Magnetic field strengths are given at 20 cm.

Elements	Pole tip field (T)	Length (m)
Quadrupoles		
Q1	0.72	0.6
Q2	0	
Q3	-0.24	
Q4	-1.25	
Q5	0	
Q6	0.78	
Sextupoles		
S1	-0.01	0.6
S2	-0.09	
S3	0.45	
S4	-1.10	
S5	1.17	
S6	-0.38	
Drifts		
L1		0.68
L2		0.2
L3		0.2
L4		0.68
L5		0.2
L6		0.2
L7		0.25

OPTICAL EFFECTS OF WEDGE DEGRADER

The coordinates used to describe the motion of particles in a beam are $\vec{z}=(x,a,y,b,l,\delta)$, where x , y are the horizontal and vertical positions of the particle, a , b are the scaled transverse momenta, l is related to the time of flight, and δ is the relative energy deviation with respect to a reference particle. The map of the energy degrader is the same as a drift, except in the coordinate δ . To second

*This work was supported by the U.S. Department of Energy, Office of Nuclear Physics, under Contract No. DE-AC02-06CH11357.

bandura@anl.gov

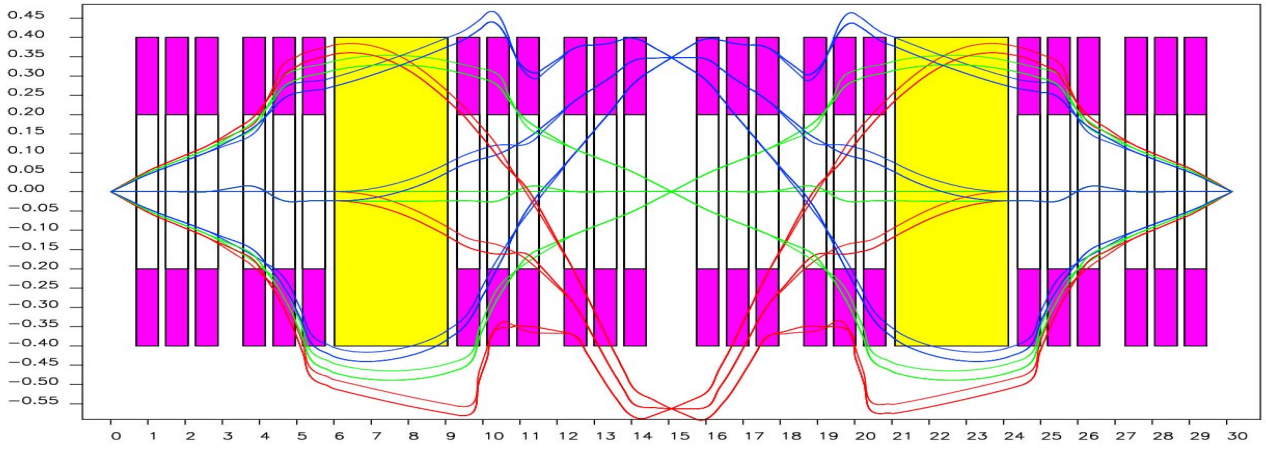


Figure 1: Fragment separator optics with beam envelope. This is an x-projection of the fragment separator. Dipoles are shown in yellow and multipoles are in pink. Lengths are given in meters. The various colors of the beam represent the same isotope with different energies.

order, the δ -component of the map can be written as

$$\begin{aligned} \delta_f &= (\delta | x)_w x_i + (\delta | a)_w a_i + (\delta | \delta)_w \delta_i + (\delta | xx)_w x_i^2 \\ &+ (\delta | xa)_w x_i a_i + (\delta | aa)_w a_i^2 + (\delta | x\delta)_w x_i \delta_i \\ &+ (\delta | a\delta)_w a_i \delta_i + (\delta | bb)_w b_i^2 + (\delta | \delta\delta)_w \delta_i^2 \end{aligned}$$

where i and f denote the initial and final coordinates, respectively.

The energy degrader should be placed at a mirror symmetric location in the fragment separator [8]. In this case we have placed it at the dispersive image. The map of the fragment separator up to this point is

$$\begin{aligned} x_f &= -x_i + (x | \delta) \delta_i + (x | xx) x_i^2 + (x | aa) a_i^2 \\ &+ (x | x\delta) x_i \delta_i + (x | yy) y_i^2 + (x | bb) b_i^2 \\ &+ (x | \delta\delta) \delta_i^2 \\ a_f &= -a_i + (a | xa) x_i a_i + (a | a\delta) a_i \delta_i + (a | yb) y_i b_i \\ y_f &= -y_i + (y | xy) x_i y_i + (y | ab) a_i b_i + (y | y\delta) y_i \delta_i \\ b_f &= -b_i + (b | xb) x_i b_i + (b | ay) a_i y_i + (y | b\delta) b_i \delta_i \\ \delta_f &= \delta_i \end{aligned}$$

To obtain the map of the whole fragment separator, one must compose the map of the first half with the map of the wedge and of the second half, which is simply the reverse of the first half.

The introduction of the energy degrader into the fragment separator causes aberrations, which may be quite large. The degrader must be shaped such that these are eliminated. To first order, the degrader must be wedge-shaped to cancel the dispersion, $(x|\delta)$, at the achromatic image of the separator. Figure 2 shows the angle necessary to eliminate dispersion for a variety of isotopes. This angle and higher order shaping, such as the curvature, depend on the energy of the beam. As the energy of the beam increases, the angle and curvature of

the wedge increase. Here we will only show plots representing a beam with energy equal to 200 MeV/u.

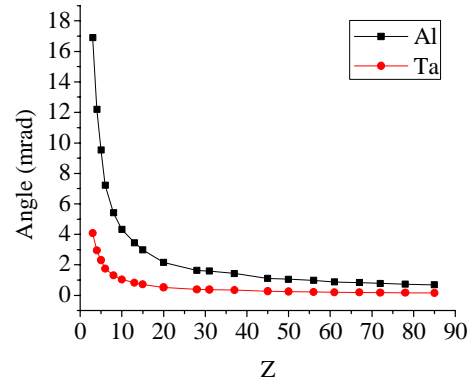


Figure 2: Angle of wedge as a function of Z at 200 MeV/u. The angle of the wedge that is necessary to cancel dispersion at the achromatic image depends on the Z of the isotope and on the degrader material.

At higher orders, the entrance and exit surfaces of the wedge can be further shaped to cancel aberrations. The second order aberrations in x that appear at the end of the separator are:

$$\begin{aligned} (x | aa)_{tot} &= (x | aa)[1 - (\delta | \delta)_w] - \frac{l_w^2}{4} (\delta | xx)_w (x | \delta) \\ &+ \frac{l_w}{2} (\delta | xa)_w (x | \delta) + (\delta | aa)_w (x | \delta) \\ (x | a\delta)_{tot} &= l_w (\delta | xx)_w (x | \delta)^2 - (\delta | xa)_w (x | \delta)^2 \\ &+ \frac{l_w}{2} (\delta | x\delta)_w (x | \delta) - (\delta | a\delta)_w (x | \delta) \\ (x | bb)_{tot} &= (x | bb)[1 - (\delta | \delta)_w] + (\delta | bb)_w (x | \delta) \\ (x | \delta\delta)_{tot} &= (x | \delta\delta)[1 - (\delta | \delta)_w] + (\delta | xx)_w (x | \delta)^3 \\ &+ (\delta | x\delta)_w (x | \delta)^2 + (\delta | \delta\delta)_w (x | \delta) \end{aligned}$$

To attain an aberration-free image at the end of the separator, however, the dispersive image should not be aberration-free. Small aberrations at the dispersive image have been shown to be advantageous. There are four aberrations that appear at the dispersive image, namely (x/aa) , (x/bb) , $(x/\delta\delta)$, and (δ/xx) . The aberration (δ/xx) is given by the curvature of the wedge. The others are determined by the second order magnetic optics. The values of the corresponding map elements are shown in Table 2.

Table 2: Transfer map elements at dispersive image. These are the transfer map elements for both a 200 MeV/u and 1500 MeV/u ^{132}Sn beam.

Map Element	200 MeV/u	1500 MeV/u
(x/aa)	-0.9	-1.9
(x/bb)	-0.9	-1.9
$(x/\delta\delta)$	-4.0	-6.2

Since it is possible from analytic theory that there may not be a universal solution for the fragment separator optics, we have investigated the effects of using different projectile-degrader material combinations. Figure 3 shows the curvature of the wedge required to cancel aberrations as a function of the projectile's nuclear charge, Z . Using an aluminum wedge, for projectiles with Z larger than about 30, the curvature stays roughly constant, with little dependence on the projectile's mass A . For lower Z projectiles there is much more variation in curvature with Z , with low Z particles having larger curvature required. There is also a dependence on A with the curvature increasing as mass increases for a given Z . As the Z of the degrader material increases, the shape of the wedge becomes less sensitive to the projectile's mass or charge. Figure 3 also shows the curvature for a tantalum wedge. While it is easy to compute the necessary curvature to cancel aberrations to second order, in practice the magnitude of the curvature is small and may be difficult to attain.

With both Al and Ta wedges, the sextupole strengths needed to cancel aberrations at the end of the fragment separator were found. The values for the sextupoles were found to be essentially constant as a function of projectile Z and degrader material. Only minor tweaking of the magnet strengths is required to focus any isotope at the end of the fragment separator. This proves the robustness of our optical layout.

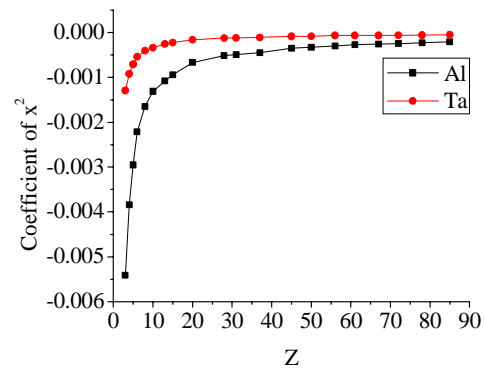


Figure 3: Curvature of wedge as a function of Z at 200 MeV/u. The curvature of the wedge depends on the Z of the isotope to be separated as well as on the degrader material.

CONCLUSION

A second order design for a fragment separator with robust optics has been developed. A design that is aberration-free to second order is preserved by appropriately shaping the wedge degrader. In order to attain this, some aberrations must be nonzero at the dispersive image. With the design presented here, at a given energy, very little tuning of the magnet strengths is needed in order to separate isotopes of varying Z and A .

REFERENCES

- [1] Y. Yano. RI Beam Factory project at RIKEN. In Proc. 17th Int. Conf. Cycl. Appl., pages 169–173, Tokyo, Japan, 2004.
- [2] W. Henning. The GSI project: An International Facility for Ions and Antiprotons. Nucl. Phys., A734:654–660, 2004.
- [3] M. Lewitowicz. Physics with SPIRAL and SPIRAL2. Status of the EURISOL project. Nucl. Phys., A734:645–653, 2004.
- [4] J. Nolen. Overview of the U.S. Rare Isotope Accelerator proposal. Nucl. Phys., A734:661–668, 2004.
- [5] B.M. Sherrill. Overview of the RIA project. NIM B, 204:765–770, 2003.
- [6] J. Symons Ed. Opportunities in nuclear science. Technical report, NSAC, 2002.
- [7] RISAC. Scientific Opportunities with a Rare-Isotope Facility in the United States. Technical report, NRC, 2006.
- [8] B. Erdelyi, J. Maloney and J. Nolen. Symmetry-Based Design of Fragment Separator Optics. (Accepted: PRST-AB)
- [9] B. Erdelyi, L. Bandura, and J. Nolen. Transfer Map Approach to and Optical Effects of Energy Degraders in Fragment Separators. (In preparation)